

# 1 INTRODUCTION

## 1.1 Background

A shock wave is a wave formed of a zone of high pressure within a fluid that propagates through the fluid at a speed in excess of the speed of sound. A shock wave is caused by the sudden, violent disturbance of a fluid, such as those created by a powerful explosion or by the supersonic flow of the fluid over a solid object. A shock wave is an extremely thin region (approximately  $0.1\mu\text{m}$ ) across which flow properties can change enormously. In general, pressure, density, temperature and entropy will increase across a shock wave, while velocity relative to the shock wave will decrease. Propagating from the point of the disturbance, a shock wave carries energy and can have destructive effects as it impinges on solid objects. A shock wave decays rapidly with increasing distance from its point of origin, gradually changing into an ordinary sound wave.

The best known examples of shockwaves are those made by the accumulation of sound waves: a balloon bursting, the crack of a fired gun, the blast of an explosion, and the sonic boom of a supersonic aircraft. At supersonic speeds, an aircraft generates numerous shock waves that emanate from major components, such as the nose, canopy, inlets, wings, and vertical tails. These multiple shock waves, seen in figure 1.1<sup>1</sup>, tend to merge into a strong bow shock and a strong tail shock as they propagate through the atmosphere. Figure 1.2<sup>2</sup> represents schlieren images of an F-18 flying at Mach 1.4 accomplished by using a schlieren camera developed by the NASA Langley Research Centre. The original image is filtered in order to decrease the banding present that is an artefact of the camera. The shockwaves emanate from the vehicle, and then begin to coalesce with each other.

---

<sup>1</sup> <http://www.slccglobelink.com/main.cfm>

<sup>2</sup> Weinstein <http://techreports.larc.nasa.gov/> (nasa.gov/centers/dryden/news/FactSheets/FS-033-DFRC.html)



**Figure 1.1: Supersonic F/A18 Hornet aircraft creates a condensation cloud as it accelerates through the sound barrier.**

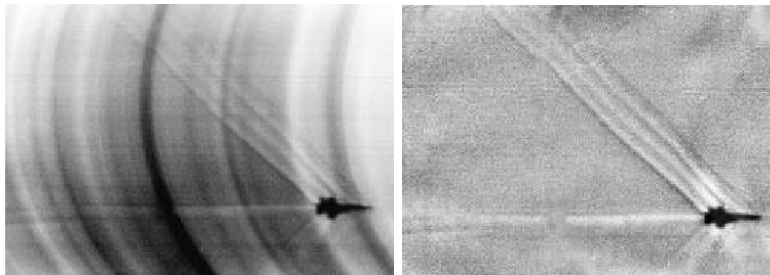


**Figure 1.2: Schlieren images of F-18 at M 1.4.**

It is common to mathematically represent a shock as a discontinuity. The relative flow in front of the shock wave will always be supersonic. The simplest form of a shock wave is a normal shock, figure 1.3. This type of shock occurs normal to a flow as a discontinuity in velocity and generally occurs over a few mean free paths. If a normal shock were propagating down a square-sectioned tube then the one-dimensional case is represented. On encountering a corner, the problem becomes two-dimensional, and if it were propagating over a wedge (corner with a width) it becomes three-dimensional.

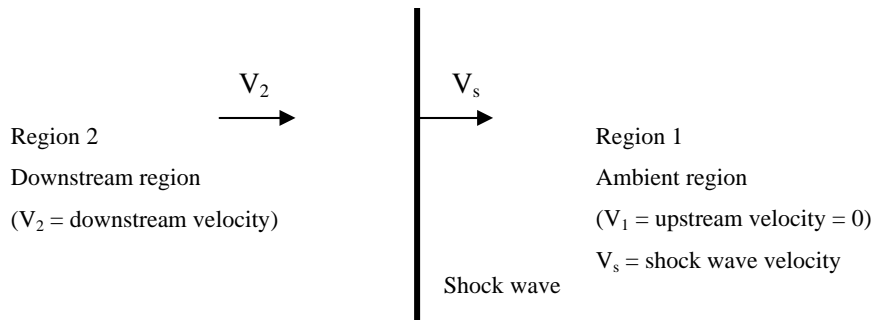


**Figure 1.3: Schematic of unsteady normal shock wave.**

## 1.2 Shock wave reflection phenomena

When an unsteady normal shock wave moving in a medium (e.g. air) interacts with another medium (e.g. a solid) obliquely, it experiences a reflection. Ernst Mach has been dubbed the first scientist to notice and record the reflection phenomena of shock waves. He reported his discovery as early as 1878. Ernst Mach recorded two different shock wave reflection configurations namely regular reflection (RR) and Mach reflection (MR).

In the early 1940's von Neumann once again commenced the intensive research of the reflection phenomena of shock waves. Since then it has been realised that the Mach reflection wave configuration can be further divided into more specific wave structures.

In general, the reflection of shock waves can be divided into regular reflection or irregular reflection (IR). A schematic drawing of regular reflection configuration is seen in figure 1.4. Two shock waves occur, namely the incident shock wave – i, and the reflected shock wave – r. The reflection point R, situated on the reflecting surface, is the point where the two waves intersect. Irregular reflections are all other reflection configurations that are obtained when an incident shock wave reflects over a surface. Irregular reflection is divided into two categories; Mach reflection and von Neumann reflection. Mach reflection is further divided into Direct-Mach reflection ( $D_iMR$ ), Stationary Mach reflection ( $S_iMR$ ) and Inverse-Mach reflection ( $I_nMR$ ). However, in general the Mach reflection configuration consists of an incident shock wave – i, a reflected shock wave – r, a Mach stem – m, one slipstream – s, a reflection point – R, as well as a

single point situated above the reflecting surface, termed the triple point - T. The reflection point is found at the foot of the Mach stem touching the reflecting surface and the triple point is where all discontinuities intersect. Figure 1.5 represents such a configuration. When the reflected shock wave – r in a Mach reflection degenerates to a compressive wave near the triple point the reflection configuration is then termed a von Neumann reflection (vNR).

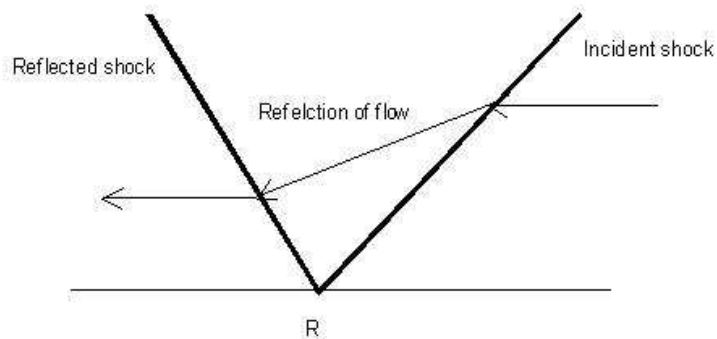


**Figure 1.4: Schematic drawing of Regular reflection configuration.**

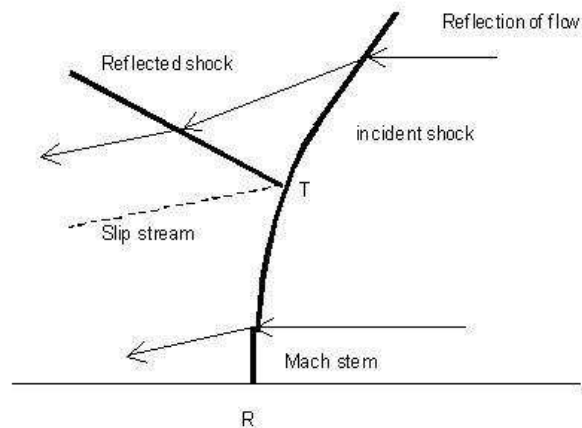


**Figure 1.5: Schematic drawing of Mach reflection configuration.**

Direct Mach reflection is found when the triple point moves away from the reflecting surface. When the triple point moves parallel to the reflecting surface a stationary Mach reflection occurs

and when the triple point moves towards the reflecting surface an inverse Mach reflection occurs. When the triple point interacts with the reflecting surface, the Inverse Mach reflection terminates to form a new wave configuration called Transitioned Regular reflection (TRR). This reflection consists basically of a regular reflection followed by a Mach reflection.

Direct Mach reflection can be divided into Single Mach reflection (SMR), Double Mach Reflection (DMR) and Transitional Mach reflection (TMR). The Single Mach reflection, as discussed before, is simply a Mach reflection. A Double Mach reflection is a Mach reflection with a kink in the reflected shock wave and the Transitional Mach reflection is a configuration between Single and Double Mach reflection.

The Double Mach reflection has two triple points. The trajectory angle of the second triple point,  $X'$ , can either be larger ( $DMR^+$ ) or smaller ( $DMR^-$ ) than the trajectory angle of the first triple point,  $X$ , depending on the initial conditions. The second triple point –  $T'$  can be found on the reflecting surface when trajectory angle of the second triple point is zero. This configuration is called a Terminal Double Mach reflection.

In summary there are ten different wave configurations that are associated with the reflection of shock waves over oblique surfaces: RR,  $\nu$ NR,  $S_t$ MR,  $I_n$ MR, TRR, SMR, TMR,  $DMR^+$ ,  $DMR^-$  AND TDMR. In steady flows Regular reflection and Single Mach reflection are possible. However, Pseudo-steady flows give rise, in addition to RR and SMR, to  $\nu$ NR,  $S_t$ MR,  $I_n$ MR, TRR, TMR,  $DMR^+$ ,  $DMR^-$  AND TDMR. Regular reflection and Single Mach reflection are of primary importance to the work outlined in this project report.

### 1.3 Literature review

Research on the three-dimensional reflection over a double wedge, where the geometry of the second wedge is actually cut into the primary wedge surface is a new idea in the field of shock wave reflection phenomenon. However, a considerable amount of research has been done on two-dimensional double wedges. Ben-Dor et al. (1987) presents analysis of shock wave configurations occurring when a plane shock is incident on a double wedge for which the second wedge may have a concave (greater) or convex (smaller) inclination than the first wedge. It is shown that there are seven different reflection processes to be expected depending on the incident shock

Mach number and the angles of the two wedges. The numerical analysis is verified with experimental shadowgraph and schlieren photographs. A shock-polar analysis of each of the seven processes was also carried out and provided information about the pressure changes and wave structures that developed immediately behind the main reflections along the wedge surfaces.

The analysis presented established all the reflection processes and final shock configurations that are possible over any double-plane-wedge combination. Figure 1.6 represents boundary lines that define seven regions with different reflection processes. Table 1.1 compliments figure 1.6. Those regions above the central diagonal are for a concave double wedge, and those below the diagonal are for a convex wedge. The analysis used the two-shock and three-shock theories of von Neumann to determine the shock wave angles and the thermodynamic properties behind the shocks for each reflection. The flow properties obtained from the solution were used to construct the relevant shock polars.

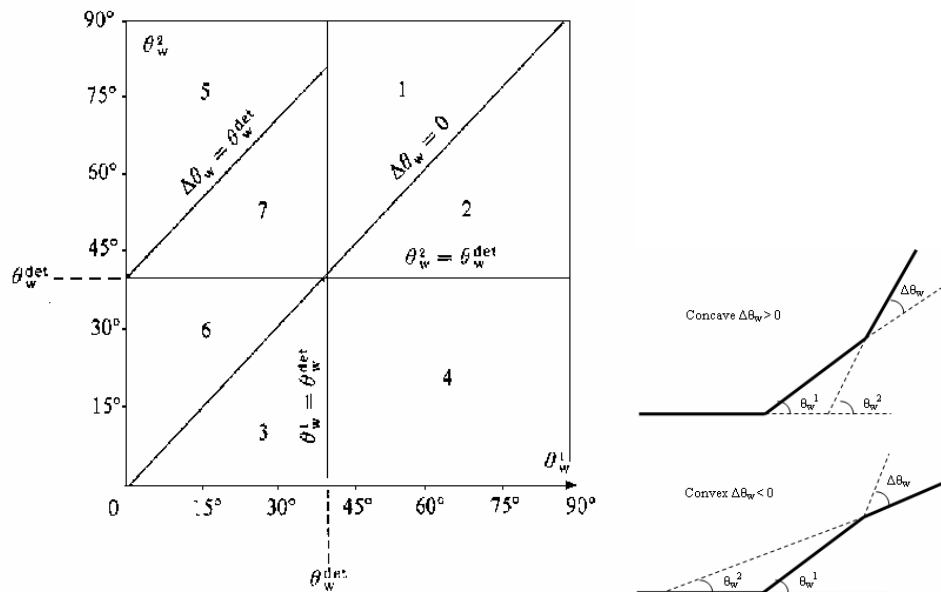


**Figure 1.6: The seven regions that identify the different reflection processes of a shock wave over a double wedge.**

$\theta_w^1$  is the first wedge angle,  $\Delta\theta_w$  the second wedge angle with respect to the first wedge angle,  $\theta_w^2$  the second wedge angle, and  $\theta_w^{\text{det}}$  the detached wedge angle corresponding to the incident shock wave Mach number  $M_i$ . The reflection processes in each region are given in Table 1.

In region 1 regular reflection was predicted over both wedges but with different wave angles. The polars that were drawn up indicated that, in general, the pressure behind the reflected shock over the first wedge will be different from the pressures behind the reflected over the second wedge, which should therefore be followed by either compression or expansion waves depending upon whether the pressure suddenly decreases or increases from the first to the second wedge. Different flow patterns were also expected behind the second reflection point according to different pressure changes.

In region 2 the reflection was expected to be regular over both wedges. It was expected that the reflection point on the second wedge would be followed by either compression waves (or a shock wave) or expansion waves depending upon whether the transition causes a sudden pressure decrease or increase. It was predicted that there are two sub-regions. In one sub-region the reflection process involves a transition from a high-pressure regular reflection to a low-pressure regular reflection. While in the other sub-region the transition is from a low- pressure regular to a high-pressure regular reflection. Therefore in the first sub-region it was expected that the reflection over the second wedge would be followed by a shock or compression wave, while in the latter sub-region it was expected that the second reflection be followed by an expansion wave.

In region 3 Mach reflection over both wedges was predicted, but with different wave angles, and a non-stationary transition region. From the shock-polars it is seen that the pressure behind the Mach stem over the second wedge will be less than that pressure behind the Mach stem over the first wedge. It was therefore expected that after the transition from the first to the second wedge, the Mach stem shock initially would be stronger than that produced by the incident shock reflection from a single wedge with the same secondary wedge angle.

In region 4 the incident shock wave was expected to reflect over the first wedge as a regular reflection and upon encountering the second wedge there is a transition to a Mach reflection. In general the pressure behind the reflected shock over the first wedge will be different from the pressure behind the Mach stem over the second wedge. A transition period was expected after the incident shock moves from the first to the second wedge with expansion or compression waves, which will dissipate through the flow.

In region 5 the incident shock was expected to reflect over the first wedge as a Mach reflection. The Mach stem of this reflection was expected to reflect over the second wedge as a regular

reflection. The triple point and the reflection point of the Mach and regular reflections interact at a point on the second wedge surface to form a new regular reflection.

In region 6 the incident shock was expected to reflect over the first wedge as a Mach reflection, and the Mach stem of this reflection reflect from the second wedge also as a Mach reflection. The triple points of these two Mach reflections intersect at a point to form a direct Mach reflection for which the triple point moves away from the second wedge surface. It was therefore expected that the Mach reflection be maintained. The changes of pressure along the wedge at the time when the triple points interact and form the third Mach reflection with a different Mach stem, was expected to result in the generation of compression or expansion waves but these are to dissipate in the flow and not persist as in regions 1 and 2.

In region 7 it was expected that the incident shock reflect over the first wedge as a Mach reflection and the Mach stem reflects from the second wedge also as a Mach reflection. Unlike the reflection in region 6, the new triple point moves towards the second wedge surface, i.e. the Mach reflection is an inverse-Mach reflection. Upon colliding with the wedge surface, the inverse-Mach reflection transitions to a regular reflection, which continues to propagate up the wedge. The shock polars drawn up suggest that a sudden pressure drop would occur from just before the termination of the inverse-Mach reflection to just after the formation of the regular reflection.

**Table 1.1: A summary of the seven different reflection processes that can occur over convex and concave double wedges.**

	$\theta_w^1$	$\theta_w^2$	$\Delta\theta_w$	First surface	Second surface	Region
<b>Convex</b>	> det	> det	-	Regular	Regular	2
<b>Convex</b>	< det	< det	-	Mach	Mach	3
<b>Convex</b>	> det	< det	-	Regular	Mach	4
<b>Concave</b>	> det	> det	-	Regular	Regular	1
<b>Concave</b>	< det	> det	> det	Mach	Regular- Regular	5
<b>Concave</b>	< det	< det	< det	Mach	Mach-Mach	6
<b>Concave</b>	< det	> det	< det	Mach	Mach- Regular	7

The reflection of plane shock waves from concave and convex double wedges was studied to establish the conditions for transition from regular to Mach reflection or Mach to regular reflection. The experimental analysis was conducted to verify the existence of the seven reflection processes predicted in the foregoing analysis as well as the predictions obtained from the shock-polar analysis. Using nominal incident-shock Mach numbers, the angles of the second wedge at which regular to Mach reflection and Mach to regular reflection occurred was determined. Observed transition wedge angles were used to modify the boundaries between regions 6 and 7, and 2 and 4 in figure 1.6, and the modification is presented as figure 1.7.

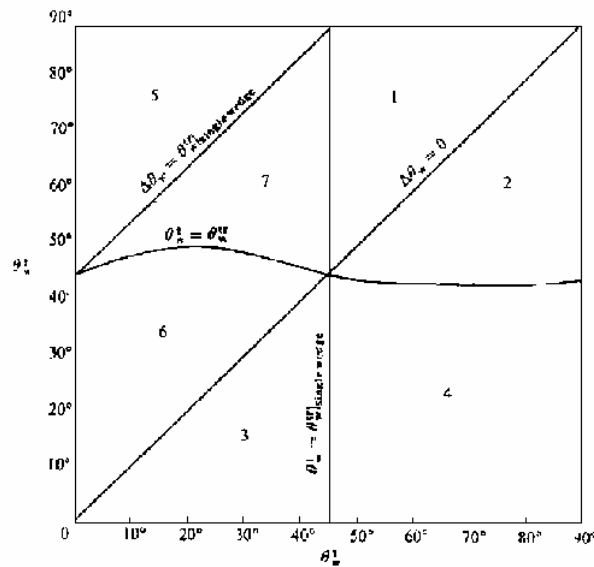


**Figure 1.7: Actual region and transition boundaries of the seven different reflection processes for an incident shock wave with  $M_1 = 1.29$  over a double wedge.**

Experimental verification of the reflection processes was carried out using combinations of wedge angles representative of each of the seven regions defined in figure 1.7, using a nominal incident-shock Mach number. The experimental verification proved that the predicted seven reflection processes did indeed exist and it was believed that the shock reflection processes described in the article are qualitatively correct.

Skews (1973) completed a two dimensional study of the reflection and subsequent diffraction of a weak shock wave interacting with a wall consisting of a concave corner followed by a convex corner. The wall angles were varied to give various combinations of regular and Mach reflection.

Convex corner angles ranging from values greater than the extreme angles through to negative values were investigated.

The situation where the reflection off both sides of the second corner C is regular is first discussed (figure 1.8a). The theory of regular reflection is well established and has been experimentally confirmed through the measurement of the shock reflection angles. Skews confirmed the prediction of the flow behind the reflected shock experimentally by examining the behaviour of points A, E, B and F during the period where the flow is pseudo-stationary. The pseudo-stationary plane was normalised and equations were developed for the resulting arcs AE and BF. For a given incident angle and shock strength the equations were solved by coupling them with the regular reflection equations. A schlieren record is included in the investigation proving in all cases agreement between theory and experimentation. From a similar analysis the distance travelled by the incident shock from the second corner to cause point B to just be overtaken by point R was calculated (limit of pseudo-stationary flow for point B) and the locus of points was then plotted with varying  $\theta_1$  from  $90^\circ$  to the catch up angle  $\theta_c$ . The results showed the whole of the reflected shock to the right of point B is pseudo-stationary irrespective of the value of  $\theta_2$ . At  $\theta_1 = \theta_c$  the flow at points A and D is pseudo-stationary as long as  $\theta_2 > \theta_c$ .

Flows where the reflection on the first wall is regular and that on the second wall is of the Mach type is discussed next (figure 1.8b). The shock behaviour is again pseudo-stationary as long as the signals from the first corner do not interfere. Skews noted that the reflected shock is stronger than the usual Mach reflection, and if this trend continued for angles close to the extreme angle then transition to regular reflection would probably occur. Skews also indicated that the reflected wave at T is stronger the lower the value for  $\theta_1$ . The strength of the reflected wave RB essentially stays constant. The length of the curved part of the shock BT was proved to increase with higher values of  $\theta_1$ . The results obtained by Skews therefore indicated that the reflected shock rather than the second wall angles is the primary factor in determining the direct motion of the triple point.

Where the reflection off the first wall is of the Mach type completes the third part of Skews' investigation (figure 1.8c). Here the flow at the second corner cannot be pseudo-stationary about this corner due to disturbances from the first corner being felt over the entire reflected shock and Mach stem. The intersection point between the sonic wave and the Mach stem will trace out a locus which will eventually intersect with the triple point locus, after which the triple point will

no longer behave in a pseudo-stationary manner. In practice the Mach reflection of a weak shock wave will always result in a curved Mach stem which will result in the locus of the sound wave interaction with stem also being curved. A segment of a curved Mach stem and the sonic intersection locus was investigated. The angle between the normal direction of the shock motion and the intersection of locus was solved once the intersection locus was found experimentally. The angle between the Mach stem and the direction of the triple point locus could then be solved, as was found to remain essentially constant on the upper portion of the curve near the triple point, implying the Mach stem is plane in this region. Experimental results showed the triple point motion remained pseudo-stationary for very much longer than suggested by the straight stem assumption.

The investigation concluded that the pseudo-stationary aspects of diffraction will no longer continue after a sufficient amount of time has passed. The motion will tend to become more complex due to the interaction of the perturbed regions arising from the two corners.

**Figure 1.8: Schematic representation of the reflection over a wall consisting of a concave followed by a convex corner: a) Regular reflection b) Mixed regular and Mach reflection c) Mach reflection**

## **1.4 Motivation**

An aircraft travelling at supersonic speed close to the ground generates a bow wave, which is reflected off the ground surface. When the aircraft enters a valley, the three-dimensional bow wave is reflected off the valley walls, such that it could focus behind the aircraft, creating a high-pressure region. Complex three-dimensional wave structures will result.

The shock wave structure over a valley is essentially a complex three-dimensional extension on the findings of the reflection on a double wedge. If one rotates the physical geometry of an aircraft entering a valley at supersonic speeds, the bow wave can approximately be represented by a planar shock wave that is incident on a wedge with a geometric cut out. Experimentally, the resulting shock wave structure can be examined by moving a planar shock wave generated from a shock tube over a geometric structure represented by cutting a relevant valley shape into a wedge at a defined angle of inclination. The resulting three-dimensional wave structures could then be identified and analysed, identifying for the first time new and innovative research on shock wave propagation into a valley.

## **1.5 Objectives**

The objective of the research is to carry out an experimental and numerical investigation on the reflection of a planar shock wave impinging on various valley and hill geometries and determining the resulting complex three-dimensional wave structures.

### **1.5.1 Experimental work**

- The objectives of the research are to be accomplished by simulating the reflection of the bow wave generated by a supersonic aircraft entering a valley in a shock tube. This will be done by moving a planar shock wave generated from a shock tube over a geometric structure represented by cutting a relevant valley shape into a wedge at a defined angle of inclination.

- Various valley geometries are to be tested in the “Seitz” shock tube at the University of the Witwatersrand, where shadowgraph and/or schlieren images are to be produced to identify two-dimensional shock reflections.
- Four different valley geometries are proposed for testing - triangular, rectangular, parabolic and conical, each of which are to be manufactured with different valley floor inclinations. These valley geometries are further cut into wedges at two different angles of inclination.
- Three different hill geometries are also proposed for the research – triangular, parabolic and conical, protruding from wedges of one inclination angle.
- The valley geometry's are to be investigated at an incident shock Mach number of 1.4.

### **1.5.2 Numerical work**

- The Computational Fluid Dynamics package FLUENT is used for three-dimensional numerical analysis of the investigated flow.
- Two- and three-dimensional numerical analysis is to be carried out on all test geometries.
- Slices through the y-z and x-y planes must be generated to investigate the reflection phenomena on the valley surfaces in two-dimensions.
- Images must be generated to investigate the resulting complex three-dimensional wave structures.

### **1.5.3 Comparison of experimental and numerical work**

- The experimental work is to be verified by comparing the schlieren images obtained through experiment to the two-dimensional images obtained through Computational Fluid Dynamics analysis.

- The resulting wave structures are to be modelled using a NURBS package RHINO giving a clear three-dimensional representation of the reflected shock surfaces.